Adaptive Wavelet Transform Techniques for Optimal Noise Reduction in Computed Tomography Scans

Lassaad Ben Ammar
Prince Sattam bin Abdulaziz University, Saudi Arabia | University of Sfax, Tunisia
l.benammar@psau.edu.sa (corresponding author)

Received: 6 October 2025 | Revised: 8 November 2025 and 7 December 2025 | Accepted: 9 December 2025

 DOI: https://doi.org/10.48084/etasr.15340

ABSTRACT

Computed Tomography (CT) often suffers from an inevitable increase in image noise due to the pursuit of reduced dose radiation, which compromises diagnostic quality and makes the detection of subtle features challenging. Conventional noise reduction methods often face a trade-off between effectively suppressing noise and preserving crucial fine-scale anatomical details and sharp edges. This paper presents an advanced denoising approach using the Adaptive Wavelet Transform (AWT) to obtain optimal noise reduction in CT scans while maintaining high image fidelity. The proposed method employs the multi-resolution decomposition property of the wavelet transform to separate noise (typically residing in high-frequency detail coefficients) from image structures (present across all sub-bands). An adaptive thresholding strategy is introduced to adjust the coefficient shrinkage based on the Genetic Algorithm (GA), thereby ensuring an effective balance between noise suppression and structural detail preservation. The proposed approach was rigorously evaluated on a publicly available dataset, comparing its performance with standard fixed-threshold wavelet methods and conventional spatial domain filters. Quantitative results demonstrate that the proposed method achieves superior PSNR and SSIM while preserving fine structural information that is vital for clinical diagnosis.

Keywords-discrete wavelet transform; adaptive threshold optimization; image denoising; adaptive algorithm

I. INTRODUCTION

In modern medical diagnostics, Computed Tomography (CT) plays a crucial role in the detection of conditions such as tumors, vascular diseases, and bone fractures [1]. If these images are corrupted by the presence of noise, then it would be harder for radiologists and clinicians to accurately interpret them and diagnose medical conditions. Therefore, performing a preprocessing step to remove noise without losing the essential anatomical details of the original image is a challenging task that aims to improve the overall quality [2]. Addressing this problem has been dealt with using various techniques ranging from traditional spatial filtering methods to more advanced techniques that incorporate mathematical transforms or Deep Learning (DL) models [3].

Spatial filtering methods adjust the values of the pixels based on their surrounding neighbors, helping to reduce unwanted variations and smooth out noise [4]. Spatial filtering can be broadly divided into two categories: linear filtering and nonlinear filtering. Linear filters (e.g., Mean and Gaussian) operate by performing a convolution operation, where a filter kernel is applied to the image pixels to modify their values based on the surrounding pixels. Since they cause blurring of the image and simultaneously suppress the details, their performances are not satisfactory. Nonlinear filters usually help avoid this problem, being more algorithmic in nature, which explains why they are named nonlinear. The median filter is one of the most common nonlinear filters that replaces the value of a pixel with the median value of intensities in its neighborhood [5]. Its performance is remarkable, especially for images with salt and pepper noise. For other types of noise, the problem of blurring edges remains challenging. Other types of nonlinear filters, such as bilateral [6] and anisotropic [7], are computationally expensive and require careful tuning of their parameters, which can be challenging in practical applications. Recent studies, such as [8-10], highlight the effectiveness of adaptive nonlinear filtering strategies in achieving significant noise suppression while maintaining the structural fidelity of medical images.

Transform domain methods convert an image from its spatial to the frequency domain using mathematical transforms, such as the Fourier or Wavelet transform. In this conversion, the image is typically decomposed into different frequency or scale components [11, 12]. High-frequency components are more likely to contain noise. Thus, thresholding or shrinking these components allows noise removal while preserving important features [13]. Despite their performance, some challenging tasks remain, with the most common related to the choice of the optimal threshold, as it can result in loss of important features or insufficient noise removal.

Recently, DL models have gained widespread adoption in medical image analysis tasks such as cancer diagnosis [14] and image denoising [15-18]. Image denoising DL models learn complex patterns of noise and image content from labeled datasets containing both noisy and clean image pairs. After that, the model can predict the clean image by estimating the noise in the new unseen image and removing it. Although DL models offer powerful solutions to image denoising, their adoption in clinical practice is hindered by several challenges, including the need for large annotated datasets (pairs of noisy and clean images) and the computational costs. Moreover, their ability to simultaneously capture both high-frequency subtle details required for early-stage diagnosis and low-frequency global structural changes indicative of severe disease remains challenging.

None of the previously mentioned methods can be universally better. Criteria such as edge preservation, data requirement, speed, and interpretability should be considered when selecting a denoising method. Table I presents a comparison of the methods mentioned for CT scan denoising.

TABLE I. COMPARISON OF DENOISING METHODS FOR MEDICAL IMAGES

Method	Edge preservation	Data requirement	Speed	Interpretability
Spatial filter	Poor	None	Fast	Transparent
Wavelet transform	Excellent	None	Fast	Transparent
DL	Excellent	High	Slow	Black-Box

This study argues that the wavelet transform presents the best trade-off regarding cost-effectiveness and computational complexity. However, a critical limitation persists due to the use of a non-optimal strategy to select the mother wavelet or the threshold value, which is often set using heuristic rules. Therefore, the performance of the denoising method is heavily dependent on the choice of wavelet and threshold type. Using adaptive methods has shown promising results compared to traditional techniques. To the best of our knowledge, this challenge is often resolved using manual tuning of the threshold value. Thus, this study presents a wavelet denoising method that leverages the Genetic Algorithm (GA). The aim was to mitigate the fixed-rule strategy used in the traditional wavelet-based denoising method through the application of GA. The latter will explore the solution space to find the optimal or near-optimal solution based on well-known quality measures, such as Peak Signal-to-Noise Ratio (PSNR) and/or Structural Similarity Index (SSIM).

II. IMAGE DENOISING BY WAVELET TRANSFORM

The wavelet transform is a powerful tool for image processing, having gained considerable attention due to its ability to efficiently represent both high-frequency and low-frequency components of an image. Image denoising using the wavelet transform consists of three basic steps: decomposition, thresholding, and reconstruction.

First, a wavelet decomposition is applied, allowing to decompose the image into four sub-bands as shown in Figure 1. The sub-band LL is derived by applying a low-pass filter to the image. It contains the low-frequency components of the image, capturing its general structure or "rough outline". This explains why it is called approximation coefficients. The sub-bands LH, HL, and HH represent the high-frequency details of the image, including sharp edges, textures, and noise, called detail coefficients. To obtain the next level of wavelet coefficients, the decomposition is further applied on the LL sub-band alone.

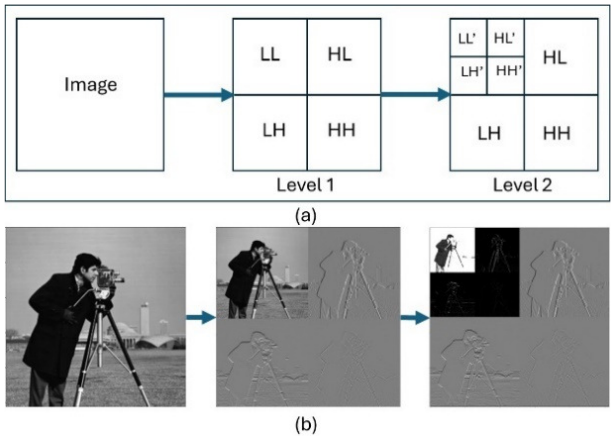

Fig. 1. Wavelet decomposition of a cameraman image: (a) First- and second-level 2D decomposition, (b) Wavelet transforms at Levels 1 and 2.

The coefficients obtained in the first step are modified by applying a thresholding technique to selectively filter out noise. To do so, a threshold value is chosen based on common methods such as Universal, SURE, or Bayesian [13]. The threshold often depends on an estimate of the noise level in the image, which is commonly derived from the detail coefficients, as the noise is expected to dominate there. For example, in universal thresholding, the estimated level of the noise is defined as the Median Absolute Deviation (MAD) of the detail coefficients at the finest level (the highest frequency) of the wavelet decomposition. Once the threshold is defined, one of the following thresholding techniques is applied: hard or soft thresholding. In both strategies, the coefficients smaller than the threshold are set to zero. Other coefficients remain unchanged in hard thresholding or are reduced by the threshold value in soft thresholding.

$$\begin{cases} hard(\mathrm{W_{i,j}}) = soft(\mathrm{W_{i,j}}) = 0, \ for \ |\mathrm{W_{i,j}}| < \lambda \\ hard(\mathrm{W_{i,j}}) = \mathrm{W_{i,j}}, \ for \ |\mathrm{W_{i,j}}| \geq \lambda \\ soft(\mathrm{W_{i,j}}) = sign(\mathrm{W_{i,j}}) * \max(0, |\mathrm{W_{i,j}}| - \lambda), \ \text{for } \mathrm{W_{i,j}} \geq \lambda \end{cases}$$

where i and j denotes the location of coordinates of the pixel, w represents wavelet coefficients, λ denotes the threshold value, and $sign$ gives the sign of the coefficient (i.e., positive or negative).

Finally, the desired image is reconstructed by applying an inverse wavelet transform to the processed coefficients. Note that, while denoising an image via wavelet transform, finding an optimum threshold that balances noise removal and feature preservation is a critical step. The threshold determines the wavelet coefficient to be retained and those to be discarded or shrunk, thereby influencing the quality of the denoised image.

A small threshold value will retain the noisy coefficients, whereas a large threshold value leads to the loss of coefficients that carry image signal details. Hard thresholding may be considered better than soft thresholding regarding edge and detail preservation. However, it can create artifacts or discontinuities in the image due to abrupt changes, especially at the threshold. On the other hand, soft thresholding usually produces smoother results with less visible noise but may slightly blur edges due to the shrinkage of all coefficients above the threshold. This challenge was the main motivation for this work.

III. PROPOSED METHOD

This section details the proposed approach for leveraging an adaptive algorithm with a wavelet transform to denoise CT scan images (Figure 2). The approach goes through three stages. In the first stage, the Discrete Wavelet Transform (DWT) is applied to effectively decompose an image into various frequency bands while preserving important details. The second stage represents the main contribution, blending a Genetic Algorithm (GA) with the thresholding technique to tune the threshold value. Once the optimal threshold value is obtained, the wavelet coefficients obtained in the first stage will be the subject of a thresholding operation. Finally, an inverse wavelet decomposition is applied to the processed coefficients to reconstruct the denoised image.

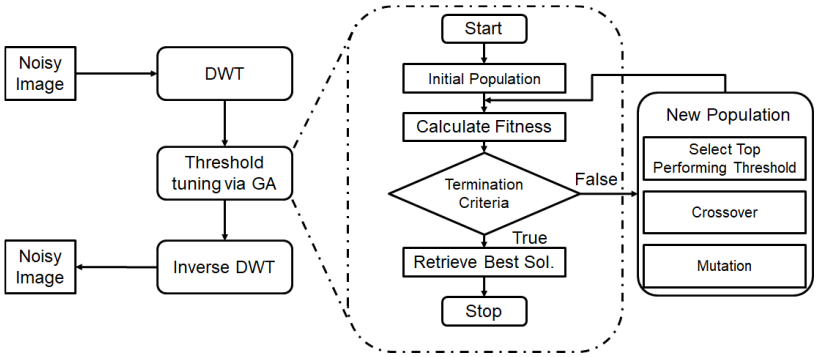

Fig. 2. Flowchart of the proposed approach for adaptive Wavelet-based image denoising.

A. Adaptive Algorithms for Threshold Optimization

The Genetic Algorithm (GA) has been largely adopted in medical image processing as an optimization technique in several tasks, such as feature extraction [14]. This study employed the GA to select the optimal threshold value to be used during the reverse process of the wavelet transform. The goal is to improve the performance of the denoising method and thus enhance the overall quality of the input image. Algorithm 1 presents the basic steps that followed for image denoising.

```
Algorithm1: Adaptive Wavelet Transform
Image Denoising
Input: Noisy Image
Output: Desired Image
1:  Coefficients ← DWT(Noisy Image)
2:  Threshold ← Estimate_Noise(NoisyImage)
3:  Population ←
      Create_population(Threshold)
4:  Repeat
5:    For each individual
6:      Calculate Fitness
7:      Select the best value
8:  Until Terminate_condition
9:  Apply thresholding to wavelet
    coefficients
10: Reconstruct the image from the
    processed coefficients
```

1) Generation of Wavelet Coefficient and Threshold Calculation

The procedure starts by decomposing the noisy image using DWT to obtain the wavelet coefficients. Afterwards, an estimate of the noise is calculated and considered as the initial threshold value that will be used to generate the initial population for the GA. Different methods can be used to estimate the noise of an image, depending on the type of noise that arises in such an image. For images corrupted by Poisson noise, the noise variance is proportional to the signal strength, and is usually adopted to estimate the noise level. CT scans are often affected by Poisson noise, which arises due to the inherent statistical fluctuations in the number of X-ray photons that reach the detector during image acquisition. Hence, the variance of the wavelet coefficient was used to estimate the noise level in the input noisy image.

2) Population Initialization

Once the noise level is estimated, the initial population is generated by scaling the estimated noise level by random factors. This population contains a collection of candidate threshold values that will evolve over time to find the best one(s) for denoising CT scans. The population size is a key parameter that should be set in this step. A small value risks leading to premature convergence, missing a good solution, whereas a large population may lead to better exploration but considerably slower computation. In the case of CT scan images, a population size of 30-80 is usually recommended to get the best trade-off between cost-effectiveness and

computational complexity. This process starts with the smallest value of the recommended range for the population size and increases it according to the balance between computational resources and the algorithm's ability to converge on a good solution. As the chromosome simply represents the threshold value, a good balance is obtained with a population size of 40.

3) Population Evaluation

The next step in the denoising procedure calculates the fitness function for everyone in the initial population. The fitness function is a key concept in the GA, as it evaluates how a candidate solution is fit for the problem under consideration. In this case, a high fitness score means that the image is well denoised. Thus, the denoising performance metric was considered as a fitness function. The fitness function of an individual i, $FiF(i)$, was determined as

$$FiF(i) = PSNR(original\_img, denoised\_img) + SSIM(original\_img, denoised\_img)$$

4) Individual Selection, Crossover, and Mutation

Based on their fitness, the best two individuals are selected to initiate a small repetitive process. They undergo a genetic operator known as *crossover*, where genetic information is exchanged between pairs of selected individuals to produce an offspring. The crossover rate is set to 0.8, which means that 80% of selected pairs undergo crossover. This value is chosen based on standard GA practice and empirical evidence that suggest that crossover rates in the range of 0.7 to 0.9 offer a good balance between convergence speed and solution quality. To ensure diversity in the new population and prevent premature convergence to sub-optimal solutions, offspring undergo a small change to their genetic information. The mutation rate is set to 0.05, meaning each gene in a chromosome has a 5% chance of being mutated. This rate is selected to ensure adequate genetic diversity without disrupting promising solutions. The newly generated individuals will replace old ones in the current population, and the process re-iterates until a termination condition is met, such as reaching a desired fitness level or exceeding a specified number of iterations. By the end of this process, the optimal threshold value is provided.

5) Thresholding and Image Reconstruction

In this step, the thresholding technique is applied to the wavelet coefficients. Values smaller than the obtained threshold are suppressed, while other coefficients will either remain unchanged or be reduced by the threshold according to the adopted thresholding technique. Finally, an inverse wavelet decomposition is performed on the processed coefficients to reconstruct the denoised image.

B. Evaluation Metrics for Denoising Performance

The performance of aany denoising method is usually evaluated via quantitative indicators such as the Peak-Signal-Noise Ratio (PSNR), Mean Absolute Error (MAE), Mean Square Error (MSE), and Structural Similarity Index Measure (SSIM). In [19], several CT denoising methods were reviewed, showing that PSNR, SSIM, and MSE are the most common evaluation metrics. Since the PSNR uses the MSE in its calculation formula, this study focused on PSNR and SSIM.

- PSNR is often chosen for its simplicity, interpretability, and direct relationship to the perceived quality of an image, reflecting the degree of similarity between the original and the processed image. Higher PSNR values indicate a higher quality of the denoised image. PSNR is calculated using

  $$PSNR = 10 * log_{10}(\frac{Max_I}{MSE})$$

  where Max_I represents the maximum image pixel intensity value (e.g., 255 for 8-bit images), and MSE is the mean squared error between the original and denoised images. The lower the MSE, the higher the denoising performance. MSE is given by

  $$MSE = \frac{1}{mn}\sum_{i=1}^{m}\sum_{j=1}^{n}\left(I_{i,j} - \hat{I}_{i,j}\right)^2$$

  where $I_{i,j}$ is the original image pixel value, $\hat{I}_{i,j}$ is the value of the denoised image pixel, and m and n are the dimensions of the image.

- SSIM is a perceptual metric that compares the structural similarity between the original and the denoised images by considering luminance, contrast, and structure information. It provides a more accurate assessment of image quality on how the human eye perceives image distortions. SSIM values fall between 0 and 1. Higher SSIM values indicate better image quality.

  $$SSIM(x, y) = \frac{(2\mu_x\mu_y + C_1) + (2\sigma_{xy} + C_2)}{(\mu_x^2 + \mu_y^2 + C_1) + (\sigma_x^2 + \sigma_y^2 + C_2)}$$

  where μ_x^2 and μ_y^2 are the average image intensities of x and y, respectively, σ_x^2 and σ_y^2 are the variances of the intensities of x and y, respectively, and σ_{xy} is the covariance between x and y. C_1 and C_2 are small constants to avoid division by zero (often set as 10^{-4}, both).

IV. RESULTS AND DISCUSSION

Experiments were conducted to quantitatively assess the performance of the proposed method, where CT scans were corrupted with artificial Poisson noise. The findings of the proposed method were comparatively evaluated over standard thresholding techniques using PSNR and SSIM. The experiments involved 5 CT scan images sourced from the IQ-OTHNCCD [20] lung cancer dataset. This dataset includes CT scans of patients diagnosed with lung cancer in different stages and healthy subjects. Taking into account clinical realism and relevance, the dataset reflects typical CT scan image characteristics encountered in real-world settings. The images were chosen at random to serve as evaluation samples. All CT scans were normalized to ensure uniform intensity scaling across all images. Then a Poisson noise of varying standard deviations ($\sigma = 0.04, 0.05, 0.06$) was introduced to simulate realistic noise levels encountered in medical imaging (Figure 3). This range of noise intensity allowed for testing the denoising method's effectiveness under various noise levels. The noisy images then underwent a series of transformations in which different wavelet and thresholding techniques were tested. In the implementation, the Haar wavelet transform was used to decompose and reconstruct the images, selected because of its low computational cost and its ability to preserve

sharp transitions. After applying the DWT with the Haar wavelet, the obtained coefficients were used to calculate the noise level of the noisy image. This value will be the main input for the GA to find the optimal threshold value. Once this threshold is obtained, the inverse wavelet transform is used to reconstruct the image. The proposed method was compared with the Daubechies (Db), Symlet (Sym), and Coifflet (Coif) wavelets, as shown in Table II.

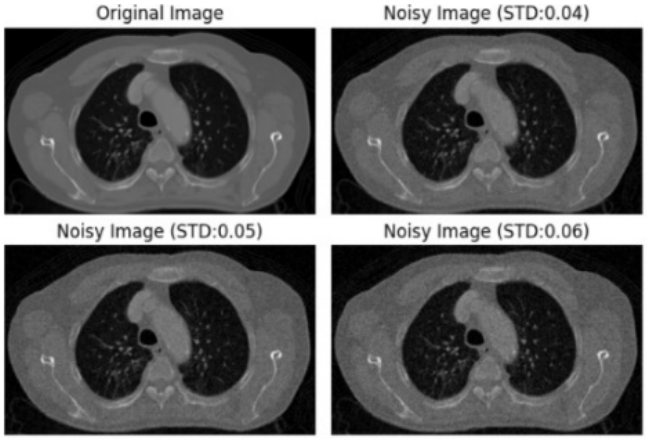

Fig. 3. Original and noisy images under varying noise levels.

TABLE II. DENOISING TECHNIQUE AND OTHER CONVENTIONAL TECHNIQUES

Noise level	Image	Metric	Noisy image	Wavelets			
				Db	Sym	Coif	Proposed
0.04	Img1	PSNR	28.43	31.69	31.80	31.94	32.66
		SSIM	0.57	0.78	0.78	0.78	0.79
	Img2	PSNR	28.36	27.10	27.15	27.21	26.71
		SSIM	0.54	0.77	0.78	0.78	0.72
	Img3	PSNR	28.49	28.64	28.63	28.76	29.80
		SSIM	0.50	0.79	0.79	0.79	0.73
	Img4	PSNR	28.38	28.23	28.23	28.32	28.96
		SSIM	0.63	0.79	0.79	0.79	0.75
	Img5	PSNR	28.29	28.43	28.61	28.76	31.34
		SSIM	0.66	0.75	0.76	0.75	0.80
0.05	Img1	PSNR	26.74	31.00	31.03	31.18	31.36
		SSIM	0.48	0.75	0.75	0.75	0.72
	Img2	PSNR	26.40	26.63	26.69	26.75	26.71
		SSIM	0.45	0.75	0.75	0.75	0.72
	Img3	PSNR	26.58	33.69	33.63	33.80	33.88
		SSIM	0.40	0.80	0.80	0.80	0.84
	Img4	PSNR	26.52	27.80	27.82	27.91	28.71
		SSIM	0.48	0.76	0.76	0.76	0.72
	Img5	PSNR	26.44	27.75	27.86	28.01	29.89
		SSIM	0.58	0.72	0.72	0.72	0.73
0.06	Img1	PSNR	24.98	29.70	29.72	29.86	29.96
		SSIM	0.41	0.70	0.70	0.70	0.74
	Img2	PSNR	23.65	25.97	26.03	26.07	26.15
		SSIM	0.34	0.69	0.69	0.69	0.65
	Img3	PSNR	23.72	31.99	31.92	32.06	33.06
		SSIM	0.28	0.74	0.74	0.74	0.80
	Img4	PSNR	23.63	27.19	27.19	27.27	28.05
		SSIM	0.36	0.70	0.70	0.71	0.67
	Img5	PSNR	23.65	26.75	26.82	26.99	27.06
		SSIM	0.46	0.67	0.67	0.67	0.60

The results show that the proposed GA-based method demonstrates superior and robust performance across diverse imagery and varying noise levels compared to fixed-threshold techniques. Moreover, the performance advantage of the GA-optimized method becomes more pronounced as the noise level increases. For low noise levels, all fixed wavelet methods are already highly optimized, and the performance gap is narrow. This confirms that the GA finds a threshold close to the VisuShrink optimum, but slightly refines it for the specific image content. As the noise power increases, the limitations of the universal (fixed) threshold become clear. The PSNR gains of the proposed method widen considerably, and the SSIM remains consistently higher.

This confirms that GA's ability to assign distinct thresholds per decomposition level prevents the overly aggressive smoothing that causes fixed methods to fail in high-noise environments. To evaluate the reliability and significance of the difference between the proposed and other techniques, a paired t-test was conducted using the obtained PSNR of each technique. The paired T-test helped determine whether the improvement observed with the proposed method was statistically significant. The results obtained indicate a statistically significant difference between the proposed and the other methods. The mean PSNR achieved by the proposed method was 28.52 dB, with a standard deviation of 4.15. For Daubechies, Symlet, and Coifflet, the mean PSNR was 26.69, 26.74, and 26.72, and the standard deviation was 3.40, 3.76, and 3.73. These results suggest that the proposed method provides a consistent and statistically significant improvement in image quality over the baseline techniques.

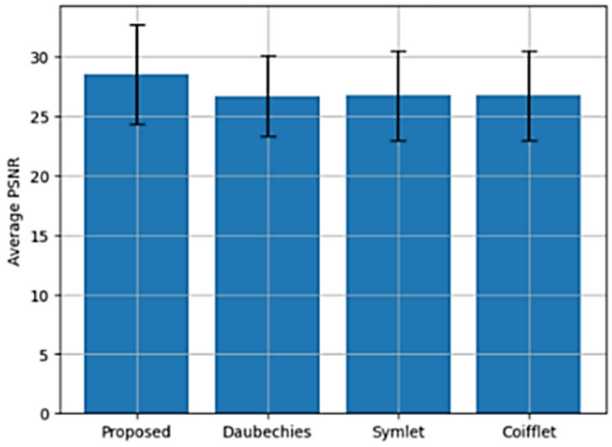

Fig. 4. Denoising performance comparison.

To contextualize the performance of the proposed wavelet-based denoising method, it was compared with three representative studies. The first employs the IQ OTH/NCCD dataset and represents the closest experimental reference [21]. Despite the hybrid wavelet-anisotropic Gaussian-CNN approach demonstrating effective noise suppression, the proposed method achieves a comparable or slightly higher PSNR, benefiting from coefficient-adaptive wavelet shrinkage that better preserves structural details. In [22], a DL-based denoiser, evaluated on a standard low-dose CT dataset, reported a higher PSNR (~31.21 dB), which can be partly attributed to the characteristics of the dataset, including cleaner

ground-truth references and more homogeneous acquisition conditions. The Transformer and CNN approach in [23], which achieved a PSNR of around 28.97 dB on another low-dose CT dataset, illustrates that even modern DL models may produce a lower PSNR under more challenging imaging conditions. These comparisons highlight that the proposed wavelet-based method delivers competitive performance across diverse datasets while maintaining a simpler architecture and reducing dependence on large-scale training data.

V. CONCLUSIONS

This study demonstrates the superiority of AWT techniques in achieving optimal noise reduction while preserving critical diagnostic information on CT scans. The proposed approach aimed to overcome the limitations of fixed-parameter wavelet methods by introducing an adaptive adjusting mechanism that tailors denoising parameters to each image's statistical characteristics. Through this adaptive optimization, the proposed method achieves an optimal balance between noise suppression and structural preservation, ensuring that diagnostically relevant features remain intact. The experimental results conclusively establish that this adaptive method yields a significantly better balance between noise suppression and structural fidelity compared to established fixed-threshold wavelet and spatial domain filters. Future work should focus on exploring hybrid models where the adaptive threshold parameters are learned via CNNs or Transformers to further refine the noise-signal classification.

ACKNOWLEDGMENT

The authors extend their appreciation to Prince Sattam bin Abdulaziz University for funding this research work through the project number (PSAU/2025/03/33627).

REFERENCES

[1] M. Diwakar and M. Kumar, "A review on CT image noise and its denoising," *Biomedical Signal Processing and Control*, vol. 42, pp. 73–88, Apr. 2018, https://doi.org/10.1016/j.bspc.2018.01.010.

[2] S. V. M. Sagheer and S. N. George, "A review on medical image denoising algorithms," *Biomedical Signal Processing and Control*, vol. 61, Aug. 2020, Art. no. 102036, https://doi.org/10.1016/j.bspc.2020.102036.

[3] R. Kaur, M. Juneja, and A. K. Mandal, "A comprehensive review of denoising techniques for abdominal CT images," *Multimedia Tools and Applications*, vol. 77, no. 17, pp. 22735–22770, Sept. 2018, https://doi.org/10.1007/s11042-017-5500-5.

[4] A. M. L. Lanzolla, G. Andria, F. Attivissimo, G. Cavone, M. Spadavecchia, and T. Magli, "Denoising filter to improve the quality of CT images," in *2009 IEEE Instrumentation and Measurement Technology Conference*, Singapore, May 2009, pp. 947–950, https://doi.org/10.1109/IMTC.2009.5168588.

[5] A. A. Omer, O. I. Hassan, A. I. Ahmed, and A. Abdelrahman, "Denoising CT Images using Median based Filters: a Review," in *2018 International Conference on Computer, Control, Electrical, and Electronics Engineering (ICCCEEE)*, Khartoum, Sudan, Aug. 2018, pp. 1–6, https://doi.org/10.1109/ICCCEEE.2018.8515829.

[6] D. Bhonsle, V. Chandra, and G. R. Sinha, "Medical Image Denoising Using Bilateral Filter," *International Journal of Image, Graphics and Signal Processing*, vol. 4, no. 6, pp. 36–43, July 2012, https://doi.org/10.5815/ijigsp.2012.06.06.

[7] Riya, B. Gupta, and S. S. Lamba, "An efficient anisotropic diffusion model for image denoising with edge preservation," *Computers & Mathematics with Applications*, vol. 93, pp. 106–119, July 2021, https://doi.org/10.1016/j.camwa.2021.03.029.

[8] M. Diwakar and P. Singh, "CT image denoising using multivariate model and its method noise thresholding in non-subsampled shearlet domain," *Biomedical Signal Processing and Control*, vol. 57, Mar. 2020, Art. no. 101754, https://doi.org/10.1016/j.bspc.2019.101754.

[9] M. Diwakar, P. Singh, and D. Garg, "Edge-guided filtering based CT image denoising using fractional order total variation," *Biomedical Signal Processing and Control*, vol. 92, June 2024, Art. no. 106072, https://doi.org/10.1016/j.bspc.2024.106072.

[10] S. Katta, P. Singh, D. Garg, V. Ravi, and M. Diwakar, "A Dual CT Image Denoising Approach using Guided Filter and method-based Noise in the NSST Domain," *The Open Bioinformatics Journal*, https://doi.org/10.2174/0118750362370719250411094442.

[11] L. Gabralla, H. Mahersia, and M. Zaroug, "Denoising CT Images using wavelet transform," *International Journal of Advanced Computer Science and Applications*, vol. 6, no. 5, 2015, https://doi.org/10.14569/IJACSA.2015.060520.

[12] J. Isabona, A. L. Imoize, and S. Ojo, "Image Denoising based on Enhanced Wavelet Global Thresholding Using Intelligent Signal Processing Algorithm," *International Journal of Image, Graphics and Signal Processing*, vol. 15, no. 5, pp. 1–16, Oct. 2023, https://doi.org/10.5815/ijigsp.2023.05.01.

[13] A. Dixit, and P. Sharma, "A Comparative Study of Wavelet Thresholding for Image Denoising," *International Journal of Image, Graphics and Signal Processing*, vol. 6, no. 12, pp. 39–46, Nov. 2014, https://doi.org/10.5815/ijigsp.2014.12.06.

[14] L. B. Ammar, "Enhanced Diagnosis of Lung Cancer through an Ensemble Learning Model leveraging an Adaptive Optimization Algorithm," *Engineering, Technology & Applied Science Research*, vol. 14, no. 6, pp. 18518–18524, Dec. 2024, https://doi.org/10.48084/etasr.9096.

[15] P. Singh and A. Shankar, "A novel optical image denoising technique using convolutional neural network and anisotropic diffusion for real-time surveillance applications," *Journal of Real-Time Image Processing*, vol. 18, no. 5, pp. 1711–1728, Oct. 2021, https://doi.org/10.1007/s11554-020-01060-0.

[16] C. Tian, L. Fei, W. Zheng, Y. Xu, W. Zuo, and C. W. Lin, "Deep learning on image denoising: An overview," *Neural Networks*, vol. 131, pp. 251–275, Nov. 2020, https://doi.org/10.1016/j.neunet.2020.07.025.

[17] S. Izadi, D. Sutton, and G. Hamarneh, "Image denoising in the deep learning era," *Artificial Intelligence Review*, vol. 56, no. 7, pp. 5929–5974, July 2023, https://doi.org/10.1007/s10462-022-10305-2.

[18] Z. Li, S. Zhou, J. Huang, L. Yu, and M. Jin, "Investigation of Low-Dose CT Image Denoising Using Unpaired Deep Learning Methods," *IEEE Transactions on Radiation and Plasma Medical Sciences*, vol. 5, no. 2, pp. 224–234, Mar. 2021, https://doi.org/10.1109/TRPMS.2020.3007583.

[19] R. T. Sadia, J. Chen, and J. Zhang, "CT image denoising methods for image quality improvement and radiation dose reduction," *Journal of Applied Clinical Medical Physics*, vol. 25, no. 2, 2024, Art. no. e14270, https://doi.org/10.1002/acm2.14270.

[20] H. Alyasriy and A. Muayed, "The IQ-OTH/NCCD lung cancer dataset." Kaggle, [Online]. Available: https://www.kaggle.com/datasets/hamdallak/the-iqothnccd-lung-cancer-dataset.

[21] T. K. Abuya, R. M. Rimiru, G. O. Okeyo, T. K. Abuya, R. M. Rimiru, and G. O. Okeyo, "An Image Denoising Technique Using Wavelet-Anisotropic Gaussian Filter-Based Denoising Convolutional Neural Network for CT Images," *Applied Sciences*, vol. 13, no. 21, Nov. 2023, https://doi.org/10.3390/app132112069.

[22] H. Zhao *et al.*, "Low Dose CT Image Denoising: A Comparative Study of Deep Learning Models and Training Strategies," *AI Medicine*, vol. 1, no. 1, Nov. 2024, Art. no. 7, https://doi.org/10.53941/aim.2024.100007.

[23] J. Zhang, Z. Shangguan, W. Gong, and Y. Cheng, "A novel denoising method for low-dose CT images based on transformer and CNN," *Computers in Biology and Medicine*, vol. 163, Sept. 2023, Art. no. 107162, https://doi.org/10.1016/j.compbiomed.2023.107162.